View metadata, citation and similar papers at core.ac.uk

brought to you by CORE

provided by Elsevier - Publisher Connector

Neuron, Vol. 45, 903–915, March 24, 2005, Copyright ©2005 by Elsevier Inc. DOI 10.1016/j.neuron.2005.02.026

Calcium-Permeable AMPA Receptor Plasticity Is Mediated by Subunit-Specific Interactions with PICK1 and NSF

Stephanie M. Gardner, Kogo Takamiya, Jun Xia,[1] Jun-Gyo Suh,[2] Richard Johnson, Sandy Yu, and Richard L. Huganir*
Department of Neuroscience
Johns Hopkins University School of Medicine
Howard Hughes Medical Institute
725 North Wolfe Street
Baltimore, Maryland 21205

Summary

A recently described form of synaptic plasticity results in dynamic changes in the calcium permeability of synaptic AMPA receptors. Since the AMPA receptor GluR2 subunit confers calcium permeability, this plasticity is thought to occur through the dynamic exchange of synaptic GluR2-lacking and GluR2-containing receptors. To investigate the molecular mechanisms underlying this calcium-permeable AMPA receptor plasticity (CARP), we examined whether AMPA receptor exchange was mediated by subunit-specific protein-protein interactions. We found that two GluR2-interacting proteins, the PDZ domain-containing Protein interacting with C kinase (PICK1) and N-ethylmaleimide sensitive fusion protein (NSF), are specifically required for CARP. Furthermore, PICK1, but not NSF, regulates the formation of extrasynaptic plasma membrane pools of GluR2-containing receptors that may be laterally mobilized into synapses during CARP. These results demonstrate that PICK1 and NSF dynamically regulate the synaptic delivery of GluR2-containing receptors during CARP and thus regulate the calcium permeability of AMPA receptors at excitatory synapses.

Introduction

The AMPA subtype of glutamate receptor mediates rapid excitatory neurotransmission in the central nervous system. The receptor is a tetramer comprised of various combinations of four basic subunits, GluR1–4, each of which can undergo alternative splicing that modifies receptor kinetics or protein interactions (Hollmann et al., 1989; Sommer et al., 1990; Song and Huganir, 2002). Furthermore, the GluR2 subunit undergoes RNA editing at a critical residue in the pore region of the subunit that controls channel properties such as ion selectivity, rectification, and polyamine sensitivity of the receptor channel. AMPA receptors that lack GluR2 are permeable to calcium, inwardly rectifying, and sensitive to polyamine block (Hollmann et al., 1991; Sommer et al., 1991; Burnashev et al., 1992; Bowie and Mayer, 1995; Donevan and Rogawski, 1995; Kamboj et al., 1995). This editing also affects the assembly of the tetramer and trafficking out of the endoplasmic reticulum (Greger et al., 2003).

The trafficking and localization of GluR2-containing receptors has been shown to involve protein-protein interactions that are regulated by protein phosphorylation events (Song and Huganir, 2002; Bredt and Nicoll, 2003; Collingridge et al., 2004). The C terminus of the GluR2 subunit is the site for several protein interactions, including a membrane proximal region of the C terminus that interacts with NSF (N-ethylmaleimide sensitive fusion protein) and AP2 (Nishimune et al., 1998; Osten et al., 1998; Song et al., 1998; Lee et al., 2002) and a PDZ ligand at the extreme C terminus which interacts with the PDZ-containing proteins PICK1 (Protein interacting with C kinase) and GRIP1/2 (glutamate receptor interacting protein) (Xia et al., 1999; Dev et al., 1999; Dong et al., 1997; Srivastava et al., 1998). Phosphorylation of a serine residue within the GluR2 PDZ ligand (Ser880) by PKC has been shown to disrupt binding of GluR2 to GRIP1/2, but has little effect on its interaction with PICK1 (Matsuda et al., 1999; Chung et al., 2000).

These two classes of interactions have been shown to be important for the membrane trafficking of endogenous as well as overexpressed GluR2-containing AMPA receptors in the forebrain (Lledo et al., 1998; Luscher et al., 1999; Luthi et al., 1999; Noel et al., 1999; Daw et al., 2000; Osten et al., 2000; Shi et al., 2001; Kim et al., 2001; Lee et al., 2002; Braithwaite et al., 2002; Terashima et al., 2004), cerebellum (Xia et al., 2000), and spinal cord (Dong et al., 1997; Li et al., 1999). The interaction of GluR2 with NSF has been shown to be necessary for maintaining synaptic AMPA receptors both basally and dynamically (Nishimune et al., 1998; Song et al., 1998 Luscher et al., 1999; Luthi et al., 1999), possibly by regulating the surface expression of GluR2, but the mechanism by which this occurs is unclear. Overexpression of PICK1 in neurons decreases the surface expression of GluR2 and suggests that PICK1 promotes the internalization of receptors or stabilizes the intracellular pools of receptors (Perez et al., 2001; Terashima et al., 2004). Moreover, PICK1 has been shown to be critical for LTD in cerebellar Purkinje cells, suggesting that the interaction of GluR2 with PICK1 can be dynamically regulated and thus modulate the synaptic level of AMPA receptors (Xia et al., 2000). PICK1 has recently been shown to have a BAR domain (Peter et al., 2004; Zimmerberg and McLaughlin, 2004), a domain found in several proteins involved in endocytosis, suggesting that PICK1 may play an active role at sites of membrane trafficking. The function of GRIP1/2 has not been well defined due to a lack of specific reagents, but appears to also be important for synaptic localization in the forebrain (Dong et al., 1997; Osten et al., 2000).

The GluR2 subunit has also been implicated in constitutive, activity-independent local cycling at hippo-

*Correspondence: rhuganir@jhmi.edu
[1]Present address: Department of Biochemistry, Hong Kong University of Science and Technology, Clear Water Bay, Kowloon Hong Kong.
[2]Present address: Department of Medical Genetics, College of Medicine, Hallym University, Chuncheon, Gangwondo, 200-702, South Korea.

campal synapses (Shi et al., 2001). In the CA1 region of the hippocampus, the incorporation of GluR2/3 heteromeric receptors into synapses has been reported to be activity independent. This is in contrast to the synaptic incorporation of GluR1/2 heteromeric receptors, which is regulated by activity (Shi et al., 2001). According to this model, the role of GluR2 in dynamic synaptic regulation is to replace the actively recruited GluR1/2 heteromers with GluR2/3 heteromers and thus allow for the maintenance in the enhancement of postsynaptic sensitivity following certain stimuli. In addition, GluR2 has been proposed to be a key subunit mediating AMPA receptor fate in recycling or degradation following internalization (Lee et al., 2004).

Recently, a form of plasticity was described at cerebellar granule cell-stellate cell synapses in which the calcium permeability of AMPA receptors is dynamically regulated (Liu and Cull-Candy, 2000; Liu and Cull-Candy, 2002). Under resting conditions, the synaptic receptor population is predominantly inwardly-rectifying calcium-permeable receptors; however, 50 Hz stimulation of the granule cell axons induces an exchange of these receptors for less-rectifying calcium-impermeable receptors, presumably by replacement of the GluR2-lacking receptors by GluR2-containing receptors. Regulation of the GluR2 content at synapses will have profound effects on the properties of synaptic responses and calcium signaling at the synapse. Since this plasticity is likely to be a common form of plasticity (Collingridge et al., 2004), we propose the term calcium-permeable AMPA receptor plasticity (CARP) to describe this process.

We sought to understand the underlying molecular mechanism of this form of plasticity by examining the regulation of the trafficking of GluR2-containing receptors in these synapses. Using a combination of intracellular peptide perfusion techniques to disrupt GluR2 protein-protein interactions and several knockout and knockin mice that alter AMPA receptor and AMPA receptor interacting protein function, we have found that PICK1 and NSF are necessary for activity-dependent changes of synaptic GluR2 content. In addition, we found that PICK1 is also important for creating extrasynaptic plasma membrane pools of GluR2-containing receptors that may be mobilized to the synapse during CARP.

Results

Intracellular Perfusion of Peptides that Disrupt GluR2 Protein-Protein Interactions Inhibit CARP

As originally reported by Liu and Cull-Candy (2000), we found that AMPA receptor-mediated synaptic currents at the parallel fiber-stellate cell synapse have nonlinear current-voltage relationships indicative of calcium-permeable AMPA receptors lacking the GluR2 subunit (Figure 1A, left). The current evoked at +40 mV is mediated predominately by GluR2-containing receptors that are not blocked by intracellular spermine, while the current evoked at –60 mV represents current through both GluR2-lacking and GluR2-containing receptors. Following high-frequency stimulation (HFS, 50 Hz), the amplitude of the synaptic responses at –60 mV decrease,

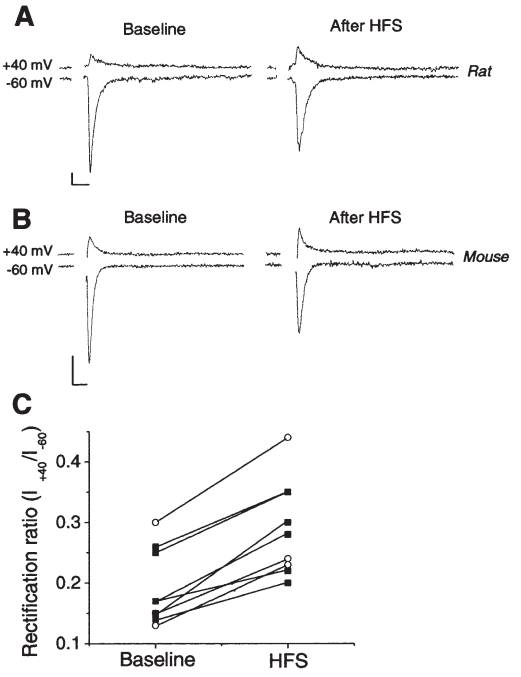

Figure 1. HFS Leads to an Increase in Synaptic GluR2

(A) (Left) Examples of inwardly-rectifying evoked synaptic AMPA receptor currents at +40 mV and –60 mV under baseline recording conditions in the rat. (Right) Following HFS, the current at +40 mV is increased and the current at –60 mV is decreased, leading to a decrease in rectification. Scale bars, 2 ms and 25 pA.

(B) (Left) Examples of baseline synaptic AMPA receptor currents in the mouse at +40 mV and –60mV. (Right) As in the rat, HFS leads to a decrease in rectification. Scale bars, 2 ms and 25 pA.

(C) Summary of rectification ratio change (post-HFS relative to pre-HFS) in stellate cells in mice (open circle) (n = 3) and rats (black square) (n = 6).

while the amplitudes at +40 mV increase (Figure 1A, right), resulting in a significant increase in the rectification ratio (I_{+40}/I_{-60}) of the evoked synaptic currents (Figure 1C). This change in rectification indicates that there is an increase in calcium-impermeable GluR2-containing receptors at the synapse. The decrease in amplitude at –60 mV is likely due to the fact that GluR2-containing AMPA receptors have a lower single-channel conductance (Swanson et al., 1997). These results suggest that there is an exchange of GluR2-containing receptors for GluR2-lacking receptors (Liu and Cull-Candy, 2000, 2002). This CARP was observed in both rats (Figures 1A and 1C) and mice (Figures 1B and 1C). On average, the percent change in the rectification ratio was 152% ± 11% in rats and 161% ± 9% in mice following HFS.

In order to determine whether intracellular protein-protein interactions with AMPA receptor subunits were involved in controlling synaptic GluR2 expression, we first performed peptide disruption experiments. A peptide designed to selectively disrupt the interaction between GluR2 and NSF (Lee et al., 2002) was included in the patch pipette, and changes in the baseline properties of synaptic AMPA receptors and the response to HFS were monitored. Peptides that disrupt GluR2-NSF

interactions have previously been shown to cause a rundown in AMPA receptor responses in hippocampal neurons (Nishimune et al., 1998; Song et al., 1998; Lee et al., 2002). Consistent with these previous results, perfusion of the NSF-specific peptide for 30 min led to a small decrease in the EPSC amplitude at +40 mV (81% ± 7% of t = 0 value, n = 5, p = 0.18); however, in contrast, the peptide had a large significant increase in the EPSC amplitude measured at –60 mV (136% ± 19% of t = 0 value, n = 5, p < 0.05) (Figure 2A). These changes in amplitude resulted in a significant decrease in the rectification ratio at 30 min compared to a control peptide (61% ± 7% of t = 0 value, n = 5, p < 0.05) (Figure 2B). These data indicate that the NSF-specific peptide has the opposite effect of HFS and causes a decrease in GluR2-containing receptors at the synapse and a compensatory increase in GluR2-lacking receptors at the synapse. No significant change in rectification was observed with a control NSF peptide (101% ± 11% of t = 0 value, n = 3, p = 0.53; amplitude at –60 mV, 95% ± 10% of t = 0 value, n = 3, p = 0.62; amplitude at +40 mV, 101% ± 5% of t = 0 value, n = 3, p = 0.97). Moreover, perfusion of the NSF-specific peptide completely blocked the HFS-induced change in the rectification ratio, indicating that CARP was severely inhibited by the NSF-specific peptide (the rectification ratio at 30 min post-HFS relative to pre-HFS was 99% ± 8%, n = 4) (Figure 2C.). NSF and the clathrin adaptor protein AP2 have recently been shown to interact with a similar region of GluR2 (Lee et al., 2002). However, perfusion of an AP2-specific peptide did not result in a significant change in the rectification ratio or current amplitudes (data not shown). These data suggest that the GluR2-NSF interaction is critical for maintaining synaptic GluR2. In addition, the interaction is important for the activity-dependent changes in synaptic GluR2 and calcium permeability of AMPA receptors.

To examine the role of protein interactions with the extreme C termini of GluR2 subunits in regulating the synaptic GluR2 content, we included small (15 amino acids) peptides containing the PDZ ligand of the GluR2 subunit in the patch pipette to disrupt GRIP1/2 and PICK1 interactions with GluR2. Three types of GluR2 peptides were initially used (see Experimental Procedures for entire sequence): a peptide (ending in SVKI) that will disrupt both GRIP1/2 and PICK1 binding, two peptides that will selectively disrupt binding with PICK1 [ending in EVKI and S(PO_4)VKI], and a control peptide (ending in SGKA) that does not disrupt PDZ interactions (Matsuda et al., 1999; Chung et al., 2000). Similar to the results with the NSF-specific peptide, perfusion of any of the three GluR2 peptides that disrupt GRIP1/2 and/or PICK1 interactions, including the peptide that selectively blocks PICK1 binding, led to a small decrease in EPSC amplitude at +40 mV [percentage of t = 0: S(PO_4)VKI, 81% ± 13% (n = 7, p = 0.45); EVKI, 70% ± 18% (n = 5, p = 0.25); SVKI, 81% ± 12% (n = 5, p = 0.36)] (Figure 3A) and an increase in the EPSC amplitude evoked at –60mV [percentage of t = 0: S(PO_4)VKI, 137% ± 13% (n = 7, p < 0.03); EVKI, 146% ± 15% (n = 5, p < 0.02); SVKI, 175% ± 41% (n = 5, p < 0.05)]. This change in current amplitude resulted in a significant reduction in the rectification ratio of 50% on average [percentage of t = 0: S(PO_4)VKI, 63% ± 9% (n = 7, p < 0.02); EVKI, 39% ± 8% (n = 5, p < 0.01); SVKI, 49% ± 6% (n = 6, p < 0.01)] (Figure 3B). Thus, these peptides, like the NSF-specific peptide, have the opposite effect of HFS and cause a decrease in GluR2-containing receptors at the synapse and a compensatory increase

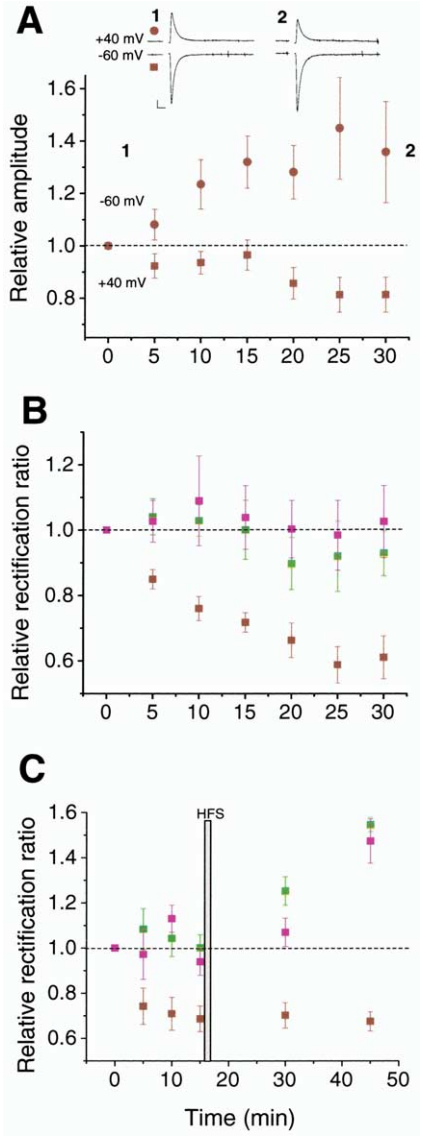

Figure 2. GluR2-NSF Interactions Are Necessary for Constitutive and Dynamic Regulation of Synaptic GluR2

(A) Perfusion of a peptide to specifically disrupt the interaction between GluR2 and NSF (200 μM) led to a significant increase in the current evoked at –60 mV (brown circle) and a small decrease in the current evoked at +40 mV (brown square) over the 30 min baseline recording period. Inset are currents from cells perfused with the NSF-specific peptide at t = 0 and t = 30. Scale bars, 2 ms and 20 pA. (B) There was a significant decrease in the rectification ratio during a 30 min recording period (n = 6). There was no change in the rectification ratio in the absence of peptide or in the presence of a control peptide (n = 7 and n = 3, respectively). (C) Disrupting the GluR2-NSF interaction blocked the increase in the rectification ratio following HFS (n = 5). NSF-specific peptide (brown square), no peptide (green square), NSF control peptide (violet square). All values are the mean ± SEM.

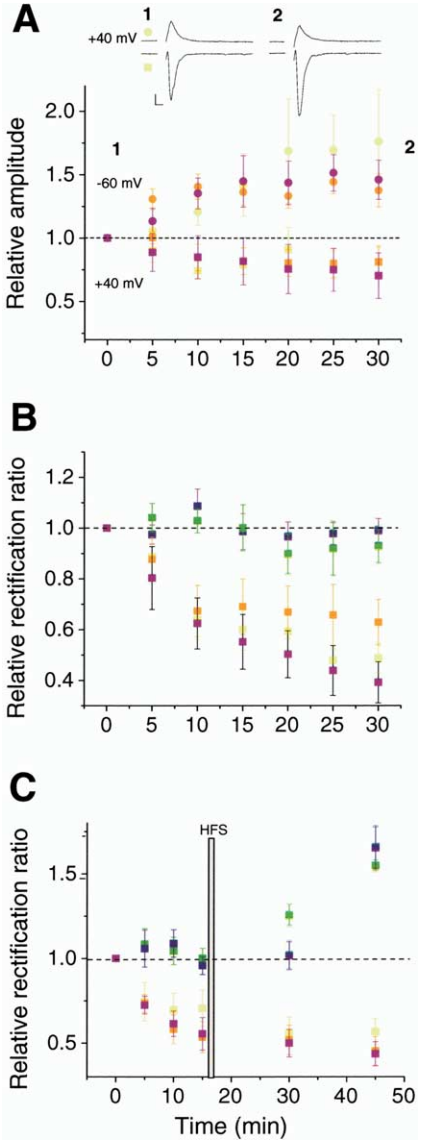

Figure 3. GluR2 PDZ Ligand Protein Interactions Are Necessary for Constitutive and Dynamic Regulation of Synaptic GluR2

(A) Disrupting PDZ interactions of GluR2/3/4c lead to a significant increase in the amplitude of the current at –60 mV and a small decrease in the current at +40 mV. Inset are currents from cells perfused with the SVKI peptide at t = 0 and t = 30. Scale bars, 2 ms and 20 pA. (B) The change in amplitude led to a significant decrease in the rectification ratio over a 30 min recording period while control peptides showed no change. Interactions with GRIP1/2 and PICK1 were disrupted with the SVKI peptide while interactions with PICK1 were disrupted with the EVKI and S(PO4)VKI peptide. (C) CARP was blocked in the presence of GluR2/3/4c C-terminal peptides [percentage of t = 15: S(PO4)VKI, 87% ± 10% (n = 6, p << 0.01); EVKI, 78% ± 3% (n = 5, p << 0.01); SVKI, 84% ± 8% (n = 6, p << 0.01)]. SVKI (yellow square), SGKA (blue square), pSVKI (orange square), EVKI (purple square), no peptide (green square). All values are the mean ± SEM.

in GluR2-lacking receptors at the synapse. Moreover, these peptides blocked the HFS-induced change in the rectification ratio, indicating that CARP was also dependent on an interaction between GluR2 and PICK1 (Figure 3C). The control peptide had no significant effect on the baseline EPSC amplitude and rectification over a 30 min recording period (percentage of t = 0: amplitude –60 mV, 96% ± 4% [n = 5, p = 0.65]; amplitude +40 mV, 94% ± 7% [n = 5, p = 0.70]; rectification ratio, 99% ± 5% [n = 5, p = 0.44]) or on the HFS-induced changes in rectification (Figures 3A–3C).

CARP Is Absent in GluR2 Knockin Mice Lacking the GluR2 PDZ Domain Ligand and in PICK1 Knockout Mice

The results of the peptide disruption experiments suggest that PICK1 interactions with the extreme C terminus of GluR2 are involved in the dynamic regulation of the GluR2 content of AMPA receptors at synapses. However, it is possible that the GluR2 peptides disrupt other PDZ domain interactions that regulate AMPA receptor trafficking. To specifically test the role of AMPA receptor trafficking in plasticity, we have generated a series of knockin and knockout mice, including knockin mice lacking the last seven amino acids of the C terminus of the GluR2 (*GluR2Δ7*) and GluR3 (*GluR3Δ7*) subunits and PICK1, GluR3, GluR4, GRIP1, and GRIP2 knockout mice (see the Supplemental Data available with this article online and Takamiya et al., 2004). All of these mice are viable except for the GRIP1 knockout mouse (Takamiya et al., 2004) and have no gross developmental defects.

In order to specifically investigate the functional role of the binding between the GluR2 C terminus and PDZ domain-containing proteins, we generated mutant mice in which the last seven amino acids of GluR2 (*GluR2Δ7*) are eliminated by introducing an artificial stop codon using knockin techniques (Figure 4A). This mutation disrupts the interaction of GluR2 with PICK1 and GRIP (Xia et al., 1999; Dong et al., 1997). An additional nonsense mutation of a BglII restriction enzyme site was introduced to verify both homologous recombination and introduction of the seven amino acid deletion (Figure 4B). Western blots of cerebellum from the *GluR2Δ7* mutant mice show that the expression of AMPA receptor subunits (GluR1–4) is not affected. However, GluR2 cannot be detected using an antibody specific for the C-terminal seven amino acids, indicating proper deletion of this region (Figure 4C). Analysis of the baseline properties of the EPSCs in the stellate cells from the *GluR2Δ7* mice showed that they were not significantly different from wild-type littermates. The average amplitude of spontaneous EPSCs (sEPSCs) in *GluR2Δ7* mice were indistinguishable from those in wild-type littermates (30 ± 4 pA versus 32 ± 2 pA for wild-type littermates [n = 4 for each], p = 0.86). There was also no significant difference in the decay kinetics of the evoked synaptic currents (τ_{decay}, 0.88 ± 0.06 ms [n = 16] versus 0.86 ± 0.09 for wild-type littermates [n = 10], p = 0.86). Paired-pulse facilitation, a measure of presynaptic release probability, did not differ between *GluR2Δ7* and wild-type littermates (P2/P1, ISI 20 ms: 1.68 ± 0.10 [n = 5] and 1.56 ± 0.06 [n = 5], respectively, p = 0.46), suggesting that presynaptic release was not affected in the knockin mice. The resting rectification ratio of the evoked EPSCs was slightly lower, although not significantly, than wild-type littermates (0.23 ± 0.02 [n = 16]

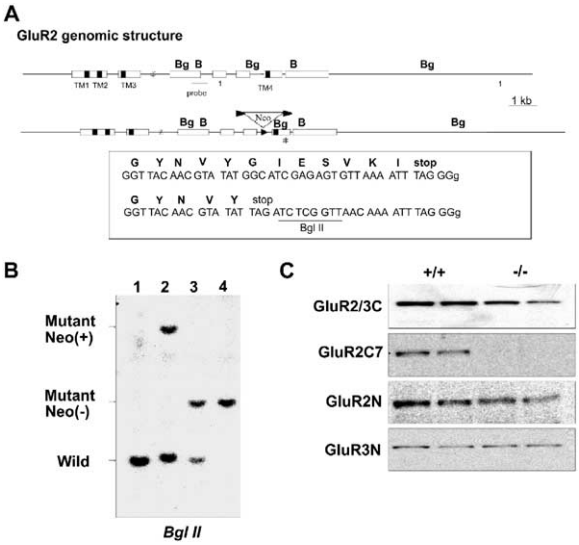

Figure 4. Generation of *GluR2Δ7* Mice

(A) Schematic representation of GluR2 mutant mouse. Genomic DNA structure of GluR2 3′ region is shown in the top panel. Exons and transembrane regions are indicated as white and black boxes, respectively. The homologous region of genomic DNA used for targeting vector is indicated by arrows. Neo^r cassette with lox-P sequences at both sides (short arrow) was introduced into BglII site in the intron upstream of the exon containing transmembrane 4 and C terminus region of GluR2. Targeted allele is indicated in the middle. After germline transmission, neo^r cassette was deleted using Cre-lox-P system by breeding to CMV-Cre transgenic mouse. The Δ7 mutation introducing the artificial stop codon and BglII site (asterisk) was generated by PCR mutagenesis. DNA and amino acid sequence are shown in detail in the box (top, GluR2 wild-type, bottom, GluR2 Δ7 mutant). Exon sequences are indicated in capital letters. TM, transmembrane; Neo, neo^r cassette; Bg, BglII; B, BamHI.

(B) Southern blot analysis of mouse genomic DNA from each step of generating mutant mice. BglII digestion of wild-type genomic DNA generates a 3 kb fragment (lane 1) and mutant genomic DNA with neo^r cassette produces a 5.5 kb fragment by destruction of the endogenous BglII site (lane 2). After neo^r cassette deletion, a 3.8 kb fragment was generated due to the introduced BglII site in Δ7 GluR2 C terminus region (lane 3, homozygous lane 4).

(C) Western blot analysis of whole cerebellum lysate. Duplicate samples were tested using various antibodies as indicated. Of special note, GluR2/3C antibody still recognizes GluR2 Δ7. On the other hand, the GluR2C7 antibody specifically recognizes the last seven amino acids of GluR2 C terminus and fails to detect GluR2 in homozygous mutant mice.

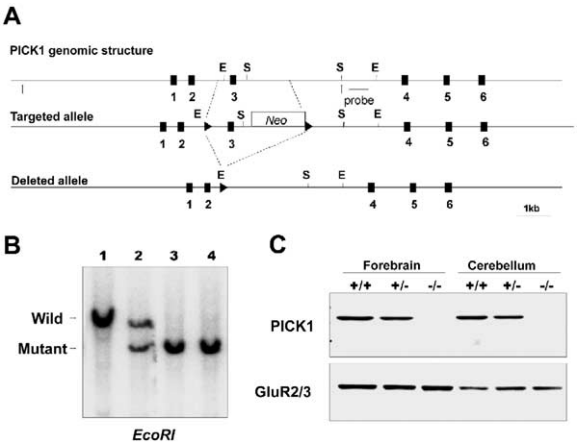

Figure 5. Generation of PICK1 Knockout Mice

(A) Conditional knockout mouse strategy was utilized in PICK1 knockout mouse generation. Neo^r cassette with one lox-P site was inserted into intron 3, and the other lox-p site was introduced into intron 2 in order to eliminate exon 3 after Cre-loxP deletion. This results in a frame-shift mutation in the PICK1 gene. The homologous region used for targeting vector is indicated by arrows (top). After homologous recombination in ES cells followed by germline transmission (middle), the floxed mice were bred to CMV-Cre transgenic mice to delete exon 3 and neo^r cassette from germline (bottom). The Cre gene was bred out of the line, as verified by PCR, and heterozygous mutant mice were intercrossed to generate homozygous mutant mice. E, EcoRI; S, SacI.

(B) Correct genotypes were confirmed by Southern blot analysis using the outside probe of targeting vector as shown in (A). The 6 kb wild-type band by EcoRI digestion of genomic DNA shifts to 5 kb due to an additional EcoRI site introduced by neo^r cassette. Lane 1, wild mouse; lane 2, heterozygous mice; lanes 3 and 4, homozygous mice.

(C) Protein samples from forebrain and cerebellum in mutant mice were tested by Western blot analysis. PICK1 signal is completely abolished in homozygous mice, while GluR2/3 expression is comparable in each genotype.

versus 0.28 ± 0.03 for wild-type littermates [n = 10], p = 0.13). These data suggest that the baseline levels of synaptic GluR2 are not significantly altered in mice whose GluR2 subunits are not able to interact with GRIP1/2 and PICK1. We next examined the dynamic regulation of AMPA receptor currents in the stellate cells by HFS. As shown in Figure 6A, following HFS, the *GluR2Δ7* mice showed no increase in the rectification ratio, indicating that CARP does not occur in these mutant mice. The rectification ratio following HFS in *GluR2Δ7* mice was 96% ± 7% of baseline compared to wild-type littermates, which showed a significant increase to 135% ± 3% of baseline. This difference in CARP was highly significant ($p << 0.01$). These results strongly support a critical role of the GluR2 PDZ ligand in the expression of CARP.

In addition to binding to GluR2, PICK1 and GRIP1/2 interact with the PDZ ligands of the GluR3 and GluR4c subunits (Xia et al., 1999; Dong et al., 1997). However, the block of CARP was specific for the far C terminus of GluR2 compared to GluR3 and GluR4c, as CARP was intact in *GluR3Δ7*, *GluR3*$^{-/-}$, and *GluR4*$^{-/-}$ mice (data not shown; see Supplemental Experimental Procedures and Figures S1–S3 for *GluR3Δ7*, *GluR3*$^{-/-}$, and *GluR4*$^{-/-}$ generation). However, there was a significant difference in the time constant of decay for currents in the *GluR4*$^{-/-}$ mice compared to wild-type littermates (1.33 ± 0.11 versus 0.92 ± 0.03 ms, n = 8 for each, $p < 0.01$), consistent the presence of GluR4 in stellate cells (Lomeli et al., 1994; Mosbacher et al., 1994).

To more directly test a role for PICK1 in the baseline and dynamic regulation of synaptic GluR2 in stellate cells, recordings were made from *PICK1*$^{-/-}$ mice and compared to wild-type littermates. PICK1 knockout mice were generated using the targeting vector for conditional knockout mice as shown in Figure 5A. After germline transmission, the exon3 and *neo* cassette were eliminated by breeding to CMV-Cre transgenic

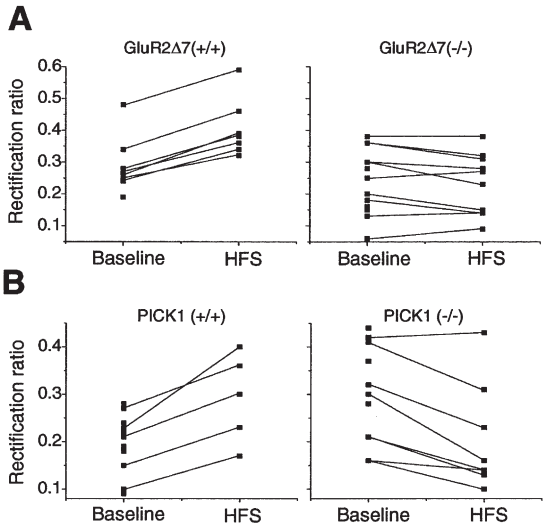

Figure 6. The GluR2 PDZ Ligand and PICK1 Are Necessary for CARP

(A) CARP is intact in wild-type littermates (left), but is absent (right) in *GluR2Δ7* mice.

(B) CARP is intact in *PICK1*$^{+/+}$ mice (left), but absent in *PICK1*$^{-/-}$ mice (right).

mice utilizing the Cre-loxP system, resulting in the introduction of out-frame mutation in the PICK1 gene. Correct homologous recombination, germline transmission, and genotype were confirmed by Southern blot using the indicated probe after PCR genotyping (Figure 5B). Western blots of hippocampus and cerebellum from the PICK1 knockout mice show that the expression of AMPA receptor subunits (GluR2/3) is not affected in the mutant mice, but PICK1 is not detected using two different PICK1 antibodies (Figure 5C). Analysis of the baseline properties of the evoked EPSC in the *PICK1*$^{-/-}$ mice showed that they were not significantly different from *PICK1*$^{+/+}$ mice. The rectification ratios were not significantly different (0.31 ± 0.02 [n = 29] and 0.27 ± 0.02 [n = 26] for *PICK1*$^{-/-}$ and *PICK1*$^{+/+}$, respectively [p = 0.17]), and the average amplitude of sEPSCs in *PICK1*$^{-/-}$ mice were indistinguishable from those in *PICK1*$^{+/+}$ littermates (29 ± 2 pA versus 28 ± 2pA for wild-type littermates [n = 4 for each], p = 0.83). There was also no significant difference in the decay kinetics of the evoked synaptic currents (τ_{decay} 0.89 ± 0.3 ms [n = 29] versus 0.91 ± 0.04 ms for wild-type littermates [n = 26], p = 0.68) or paired-pulse facilitation (1.45 ± 0.04 [n = 8], 1.61 ± 0.17 [n = 5], respectively, p = 0.19). However, as with the *GluR2Δ7* mutant mice, HFS did not increase the rectification of synaptic EPSCs in the *PICK1*$^{-/-}$ mice (rectification ratio percentage of t = 0: *PICK1*$^{-/-}$ 73% ± 6% [n = 5]; *PICK1*$^{+/+}$, 155% ± 8% [n = 8], p << 0.01) (Figure 6B), and in fact, there was a highly reproducible decrease (p < 0.01) in the rectification ratio. These results indicate that the activity-dependent regulation of GluR2 trafficking to the synapse is severely disrupted in the absence of PICK1.

Interestingly, the effect of perfusion of the GluR2 PDZ ligand peptide (SVKI) on baseline EPSCs and rectification ratio in wild-type mice described above was not observed in the *PICK1*$^{-/-}$ mice (Figure 7A: EPSC amplitude; –60 mV, percentage of t = 0: 99% ± 8% [n = 5], p = 0.90; +40 mV, percentage of t = 0: 93% ± 3% [n = 5], p = 0.42) (Figure 7B: rectification ratio; percentage of t = 0: 99% ± 5% [n = 5], p = 0.96). These results provide strong evidence that the effects we observed with the GluR2 PDZ ligand peptides were due to disruptions in the GluR2-PICK1 interaction.

NSF has been shown to regulate the interaction of GluR2 and PICK1 in vitro (Hanley et al., 2002), suggesting that PICK1 and NSF might interact in controlling synaptic GluR2. We examined whether peptides that disrupt GluR2-NSF interactions were effective in the *PICK1*$^{-/-}$ mice. Indeed, perfusion of the NSF-specific peptide had no effect on the amplitudes of evoked currents at –60 mV (percentage of t = 0: 101% ± 2%, n = 5, p = 0.88) or +40 mV (percentage of t = 0: 103% ± 5%, n = 5, p = 0.36) or rectification ratios (percentage of t = 0: 102% ± 5, n = 5, p = 53) in *PICK1*$^{-/-}$ mice recorded over a 30 min period (Figures 7C and 7D). These results suggest that in the *PICK1*$^{-/-}$ mouse there is a functional uncoupling of the NSF-GluR2 interaction that may be important for the absence of CARP in these mice.

Recordings from *GRIP2*$^{-/-}$ mice (Takamiya et al., 2004) revealed normal baseline properties of the evoked EPSC, presynaptic properties, and intact CARP following HFS (data not shown). GRIP1 knockout mice are embryonic lethal (Bladt et al., 2002; Takamiya et al., 2004), so we are unable to directly test a role for GRIP1 in regulating synaptic GluR2 in stellate cells.

Dynamin-Dependent Endocytosis Is Not Required for CARP Expression

The increase in synaptic GluR2 following HFS can result from either an increase in the insertion of GluR2-containing receptors, an increase in the removal of GluR2-lacking receptors, or a lateral movement in the plasma membrane of GluR2-containing receptors to synapses or GluR2-lacking receptors away from synapses. To dissect the general process of CARP, endocytosis was blocked and the baseline and activity-dependent changes in GluR2 content of synaptic receptors were monitored. Inclusion in the patch pipette of a peptide that disrupts the interaction between dynamin and amphiphysin to block endocytosis (Wang and Linden, 2000) led to a significant increase in the current evoked at –60 mV (Figure 8A; 148% ± 18% of amplitude at t = 0, n = 5, p < 0.02). Interestingly, there was no change in the current at +40 mV (99% ± 12% of amplitude at t = 0, n = 5, p = 0.96). The change in current amplitude at –60 mV resulted in a decrease in the rectification ratio over 30 min (Figure 8B; 64% ± 8% of t = 0, n = 5, p < 0.04). These data indicate that blocking endocytosis increases the level of GluR2-lacking receptors at synapses and has little effect on the synaptic content of GluR2-containing receptors. These results further suggest that GluR2-lacking receptors undergo a higher rate of basal endocytosis than do GluR2-containing receptors and that GluR2-containing receptors are basally introduced into the synapse at a slower rate than GluR2-lacking receptors. However, blocking dynamin-dependent endocytosis had no effect on CARP compared to no-peptide controls (rectification ratio percentage of t = 15: 152% ± 9%, n = 5, p = 0.47) (Fig-

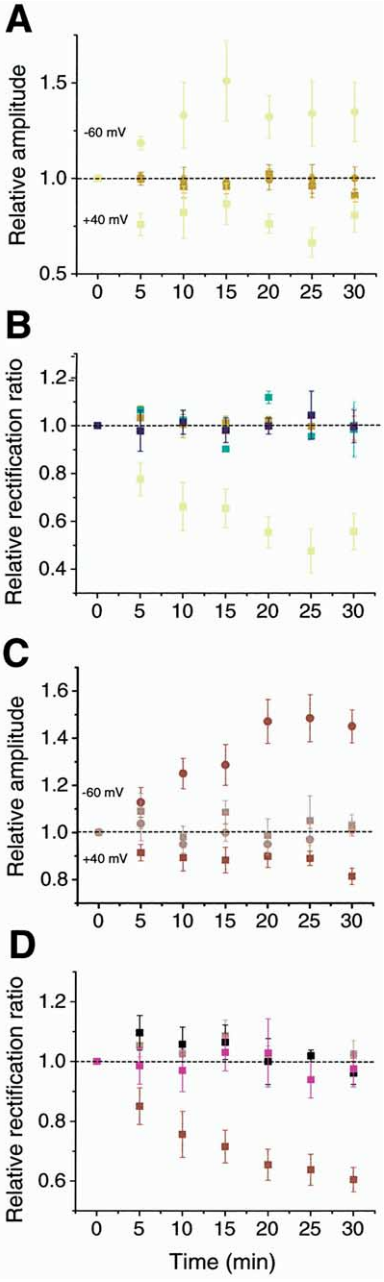

Figure 7. The GluR2 PDZ Ligand, PICK1, and NSF Are Necessary for Constitutive and Dynamic Regulation of Synaptic GluR2

(A) Perfusion of the SVKI peptide in *PICK1*$^{-/-}$ mice did not change the current amplitudes (–60 mV [rust circle], +40 mV [rust square]) or the rectification ratio (rust square) (B) over a 30 min recording period (n = 5). In *PICK1*$^{+/+}$ mice, the SVKI peptide caused significant increase in current at –60 mV (yellow circle) and a small decrease at +40 mV (yellow square) (n = 5). This resulted in a decrease in the rectification ratio (yellow square). *PICK1*$^{+/+}$ SGKA (blue square), *PICK1*$^{-/-}$ SGKA (cyan square) (n = 3). (C) Perfusion of the NSF-specific peptide in *PICK1*$^{-/-}$ mice did not change the current amplitudes at –60 mV (gray circle) and +40 mV (gray square) nor rectification ratio (gray square) (D) over a 30 min recording period (n = 5). In *PICK1*$^{+/+}$ mice, the NSF-specific peptide resulted in a significant increase in current amplitude at –60 mV (brown circle), and a small decrease at +40 mV (brown square) resulting in a significant decrease in the rectification ratio (brown square) (n = 7). *PICK1*$^{+/+}$ control peptide (violet square), *PICK1*$^{-/-}$ control peptide (black square). All values are the mean ± SEM.

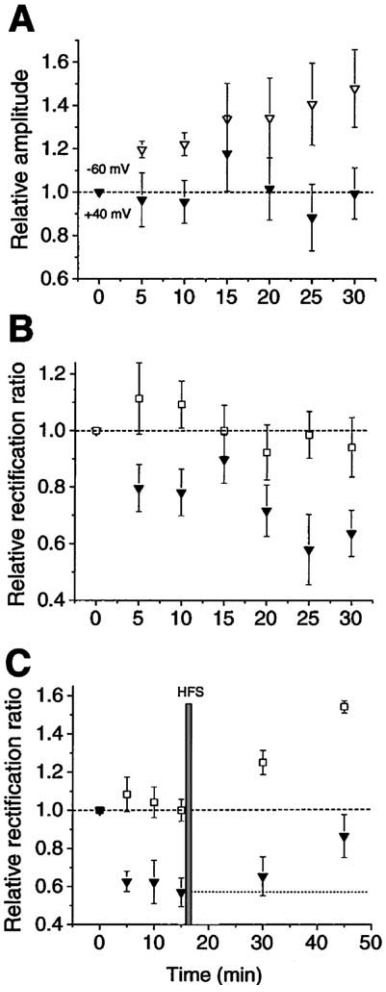

Figure 8. Dynamin-Dependent Endocytosis Is Not Required for CARP

(A) Perfusion of the dynamin peptide (black triangle) led to a significant increase in the current evoked at –60 mV, with no change in the current evoked at +40 mV over a 30 min recording period (n = 5). (B) This resulted in a decrease in the rectification ratio. There was no change in the rectification ratio in the absence of peptide (open square) (n = 7). (C) Perfusion of the dynamin peptide did not block the increase in the rectification ratio following HFS. All values are the mean ± SEM.

ure 8C). These data demonstrate that acute disruption of dynamin-dependent endocytosis of AMPA receptors is not required for CARP. However, it is possible that a prolonged disruption of endocytosis would eventually led to the disruption of CARP through depletion of recycling pools of GluR2-containing receptors. Experiments using intracellular perfusion of botulinum and tetanus toxin to test the role of membrane insertion in CARP were not successful due to a lack of an effect of these toxins on basal synaptic properties.

Extrasynaptic Plasma Membrane Pool of GluR2-Containing Receptors Is Regulated by GluR2-PICK1 Interactions

The pathway that receptors take from intracellular pools to synapses is unclear. Receptors could be in-

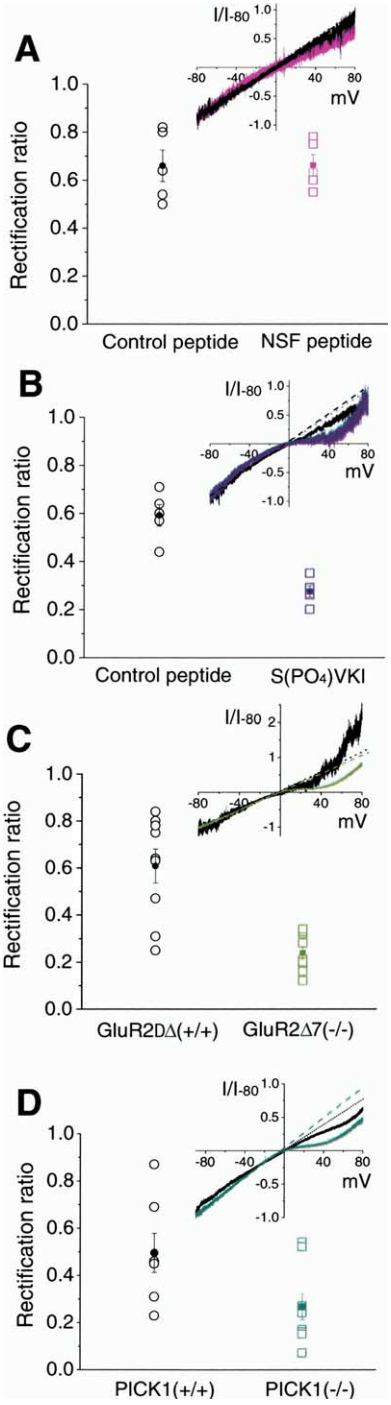

Figure 9. Locus of Action for PICK1 and NSF

(A) Disruption of GluR2-NSF interaction does not affect rectification ratios of currents from extrasynaptic AMPA receptors. (Inset) Superimposed, normalized currents evoked in response to AMPA during a voltage ramp with the NSF peptide (pink) and control peptide (black). Currents from patches in the presence of the test and control peptide were nearly linear compared to the extrapolated linear line (black dotted line).

(B) Disruption of GluR2-PICK1 with the S(PO_4)VKI peptide led to a significant decrease in the rectification ratio of extrasynaptic AMPA receptors compared to the control SGKA peptide. (Inset) Superimposed, normalized currents evoked in response to AMPA during a voltage ramp with the S(PO_4)VKI peptide (navy) and control peptide (black). Currents from patches in the presence of the test peptide showed strong inward rectification and deviated from the extrapolated linear line (navy dotted line), whereas currents from patches in the presence of the control peptide were closer to linear (black dashed line).

(C) The rectification ratios of currents from extrasynaptic AMPA receptors were significantly lower in *GluR2Δ7* mice compared to wild-type littermates. (Inset) Superimposed currents in patches from *GluR2Δ7* mice (olive trace) and wild-type littermates (black trace). Currents from *GluR2Δ7* mice show strong inward rectification and deviated from the extrapolated line at positive potentials (olive dashed line), while those from wild-type littermate were more close to linear at positive potentials (black dotted line).

(D) The rectification ratios of currents from extrasynaptic AMPA receptors in somatic patches from cells in PICK1 knockout mice were significantly different from wild-type littermates. (Inset) Superimposed currents in patches from *PICK1*$^{-/-}$ (dark cyan trace) and *PICK1*$^{+/+}$ (black trace). Currents from *PICK1*$^{-/-}$ mice show strong inward rectification and deviated from the extrapolated line at positive potentials (dark cyan dashed line), while those from *PICK1*$^{+/+}$ mice were more close to linear at positive potentials (black dotted line).

The mean ± SEM is represented as filled symbols in (A)–(D).

serted into the extrasynaptic membrane and then laterally diffuse into synapses or they could be directly inserted into synapses (Passafaro et al., 2001; Tardin et al., 2003; Groc et al., 2004). Acutely disrupting interactions between GluR2 and either PICK1 or NSF results in a loss of synaptic GluR2 in stellate cells, indicating that these interactions are critical for synaptic incorporation. The locus of these interactions, however, is unknown. If the role of NSF is indeed to disrupt the GluR2-PICK1 complex to allow for synaptic localization of GluR2 (Hanley et al., 2002), NSF could be acting to liberate GluR2 from a PICK1-tethered intracellular pool. On the other hand, NSF may be acting at an extrasynaptic plasma membrane location to allow GluR2-containing receptors to be mobilized to the synapse. To distinguish between these two possibilities, we perfused cells with the NSF-specific peptide to disrupt GluR2-NSF interactions and then examined the properties of AMPA-induced currents in the extrasynaptic membrane using excised somatic patches. As reported previously (Liu and Cull-Candy, 2000, 2002), the extrasynaptic plasma membrane of stellate cells contains an abundance of nonrectifying GluR2-containing AMPA receptors (Figure 9). Perfusion of the NSF-specific peptide had no effect on the current-voltage relationships of AMPA-induced currents in the outside-out somatic patches compared to the control peptide (Figure 9A; 0.66 ± 0.4 versus 0.66 ± 0.06, n = 5 for each), indicating that acutely disrupting NSF-GluR2 interactions does not affect the levels of extrasynaptic GluR2-containing receptors. This result suggests that NSF does not act acutely to release GluR2 from an intracellular pool to be inserted into the extrasynaptic membrane.

Disrupting the GluR2-PICK1 interaction acutely results in a loss of synaptic GluR2 in stellate cells. This may be the result of disrupting a nonsynaptic pool of GluR2 that is either intracellular or in the extrasynaptic plasma membrane. To determine the location of the GluR2-PICK1 interaction that is important for maintaining synaptic GluR2 under basal conditions, we perfused cells with the PICK1-specific disrupting peptide

S(PO_4)VKI and then examined AMPA-induced currents in isolated somatic patches. Rectification ratios of receptors in patches in the presence of the S(PO_4)VKI peptide were significantly lower than those in patches isolated after perfusion of the SGKA control peptide (Figure 9B; 0.27 ± 0.02 versus 0.59 ± 0.04, n = 5 for each, $p << 0.01$). This indicates that PICK1 is essential for getting GluR2 to the extrasynaptic plasma membrane.

It is possible that the extrasynaptic receptors may be the source of the GluR2-containing receptors that are recruited to synapses during CARP. As discussed above, the basal synaptic GluR2 content is not different between wild-type and *PICK1*$^{-/-}$ or *GluR2Δ7* mice; however, we asked if the extrasynaptic pools of GluR2 were altered in these mice. Current-voltage relationships of currents evoked with AMPA in excised somatic patches were significantly different in *GluR2Δ7* mice than those from wild-type littermates (Figure 9C; rectification ratio 0.24 ± 0.01 versus 0.61 ± 0.05 in wilde-type littermates, n = 9 for each, $p < 0.01$), indicating that there are fewer extrasynaptic GluR2-containing receptors in the *GluR2Δ7* mice than in wild-type mice. Similarly, current-voltage relationships of currents in excised somatic patches were significantly different in the *PICK1*$^{-/-}$ mice compared to wild-type littermates (Figure 9D; rectification ratio 0.27 ± 0.05, n = 9, versus 0.50 ± 0.08, n = 7, in *PICK1*$^{+/+}$, $p < 0.03$). These data strongly suggest that the level of extrasynaptic GluR2-containing receptors is low in the *PICK1*$^{-/-}$ or GluR2Δ7 mice. Confirmation of this conclusion at the morphological level using immunocytochemical analysis would involve the quantification of the extrasynaptic levels of GluR2 using immunogold EM techniques. Unfortunately, this would be extremely difficult, if not impossible, because of the sparse distribution of stellate cells in the cerebellum and the fact that they are intermingled in the molecular layer with the more abundant Purkinje cell dendrites. However, the experiments described above using peptide disruption of the GluR2-PICK1 interactions and the *PICK1*$^{-/-}$ or GluR2Δ7 mice strongly support the idea that that GluR2-PICK1 interactions are important in maintaining extrasynaptic GluR2 content. Furthermore, these results suggest that deficit in CARP in the *PICK1*$^{-/-}$ and *GluR2Δ7* mice may be, in part, attributable to a decrease in the extrasynaptic pool of GluR2 that serves as a source of calcium-impermeable AMPA receptors for synapses.

Discussion

Many forms of synaptic plasticity in the brain have been shown to be a result of either an activity-dependent increase or decrease in the number of synaptic AMPA receptors that is, in part, due to modulations of AMPA receptor phosphorylation state and protein-protein interactions (Song and Huganir, 2002; Bredt and Nicoll, 2003). For example, in hippocampal pyramidal cells the majority of AMPA receptors are calcium impermeable and consist of GluR1/2 or GluR2/3 combinations (Wenthold et al., 1996). In these cells, the synaptic insertion of GluR2/3 receptors have been reported to be part of an unregulated, constitutive pool of receptors, whereas the synaptic incorporation of GluR1/2 receptors are thought to be involved in an activity-dependent pathway that underlies hippocampal LTP (Shi et al., 2001; Passafaro et al., 2001). In cerebellar stellate cells, there exists a distinct form of plasticity that does not involve a simple change in the density of receptors, but rather an apparent change in receptor subunit composition, which results in changes in the calcium permeability of synaptic receptors (Liu and Cull-Candy, 2000, 2002). The level of calcium-impermeable AMPA receptors at these synapses is regulated by the intrinsic spontaneous synaptic activity, and HFS can lead to a rapid increase in the synaptic content of calcium-impermeable receptors (Liu and Cull-Candy, 2000, 2002). Since the GluR2 subunit determines the calcium impermeability of AMPA receptors, this plasticity is thought to occur through the dynamic exchange of GluR2-lacking and GluR2-containing receptors at the synapse. At the molecular level, this exchange of receptor subtypes could be mediated by modulating the trafficking of either the GluR2-containing or GluR2-lacking receptors, or both. We report here that the interaction of the NSF and PICK1 proteins specifically with the GluR2 subunit is essential for CARP, indicating that the trafficking of GluR2-containing receptors controls the receptor subtype exchange. Our findings suggest that, in contrast to CA1 hippocampal pyramidal cells, interactions with the GluR2 subunit are required for activity-regulated incorporation of AMPA receptors into synapses.

This difference in the regulation of AMPA receptors in the hippocampus and the cerebellar stellate cells may be due, in part, to the AMPA receptor subunits expressed in these cells. In contrast to the hippocampal pyramidal cells, cerebellar stellate cells contain little GluR1 (Baude et al., 1994; Petralia et al., 1997) and have calcium-permeable and -impermeable AMPA receptors, which most likely consist of GluR3/4 and GluR2/3 combinations, respectively. Here we show that GluR2 interactions with PICK1 and NSF are required for both the constitutive and regulated trafficking of GluR2-containing AMPA receptors that occurs during CARP. While GluR3 and GluR4c have been shown to interact with PICK1 (Xia et al., 1999; Dong et al., 1997), these interactions do not appear to be important for the baseline GluR2 content of synaptic AMPA receptors, nor are they involved in CARP, as both of these properties are normal in *GluR3Δ7*, *GluR3*$^{-/-}$, and *GluR4*$^{-/-}$ mice. Our data strongly implicate that protein interactions with the PDZ ligand of the GluR2 subunit alone are important for determining basal content and activity-dependent changes in synaptic and extrasynaptic GluR2. Our data also show that GluR2 interactions with NSF are necessary for synaptic GluR2 content but do not regulate the pools of extrasynaptic GluR2-containing receptors. These results suggest that NSF regulates the lateral mobility of extrasynaptic receptors into the synapse as has recently been shown in cerebellar Purkinje cells (Steinberg et al., 2004).

We have previously found that GluR2 interactions with PICK1 are also critical for the expression of LTD in cerebellar Purkinje cells (Xia et al., 2000). This form of LTD is induced by the activation of PKC and is mediated by the removal of synaptic AMPA receptors

through clathrin-dependent endocytosis (Wang and Linden, 2000). We have shown that this form of LTD requires the phosphorylation of AMPA receptors on the GluR2 subunit at Ser-880 within its C-terminal PDZ ligand (Chung et al., 2003) and the interaction of the GluR2 subunit with PICK1 (Xia et al., 2000). We proposed a model based on these findings wherein PICK1 binds GluR2 following PKC-mediated phosphorylation at Ser-880 and facilitates endocytosis of GluR2-containing AMPA receptor complexes, or alternatively, stabilizes GluR2-containing AMPA receptors in intracellular pools (Chung et al., 2003). How could PICK1 be involved in both the activity-regulated delivery of GluR2-containing receptors in cerebellar stellate cells and in the activity-dependent removal of GluR2-containing receptors in cerebellar Purkinje cells? One possible explanation is that PICK1 may act in a bidirectional manner that is differentially regulated by protein phosphorylation/dephosphorylation. We hypothesize that PICK1 may tether pools of GluR2-containing receptors at nonsynaptic sites, either extrasynaptic or intracellular pools, and that the dynamic regulation of GluR2 interaction with PICK1, possibly through phosphorylation/dephosphorylation of GluR2, can up- or downregulate the level of synaptic AMPA receptors. Thus, PICK1 could decrease synaptic AMPA receptors by increasing its interaction with GluR2 or increase synaptic AMPA receptors by decreasing its interaction with GluR2. In cerebellar Purkinje cells, PKC phosphorylation of GluR2 is critical for LTD expression (Chung et al., 2003) and it is possible that protein dephosphorylation of GluR2 is critical for the expression of CARP in cerebellar stellate cells.

We propose a model for GluR2 synaptic trafficking where PICK1 is involved not only in internalization and stabilization of intracellular GluR2-containing receptors (Kim et al., 2001; Terashima et al., 2004; Xia et al., 2000), but also in their cycling to the extrasynaptic membrane and the synapse (Daw et al., 2000) (Figure 10). The interaction of GluR2 with PICK1 would form an extrasynaptic pool of calcium-impermeable AMPA receptors at both intracellular and extrasynaptic plasma membrane sites, which could be recruited to synapses upon HFS. NSF would be critical for this recruitment, as it would regulate the dissociation of GluR2-PICK1 complexes during CARP, releasing GluR2-containing AMPA receptors from the extrasynaptic membrane, allowing them to diffuse laterally to the synapse (Hanley et al., 2002). This model predicts a new role for PICK1 in getting GluR2-containing receptors to the extrasynaptic membrane where they can either be internalized or recruited to the synapse. The relative rates of internalization and movement to the synapse will be regulated by synaptic activity and presumably by the balance of protein phosphorylation/dephosphorylation events in the cells.

How does CARP differ from more classic forms of plasticity such as LTP and LTD? Modulation of the proportion of GluR2-containing, calcium-impermeable AMPA receptors at synapses will not only alter the amplitude of synaptic responses but also will modify the characteristics of the postsynaptic depolarization and the activation of calcium-dependent intracellular signaling pathways. GluR2-lacking, calcium-permeable AMPA receptors have a larger single-channel conductance than GluR2-containing AMPA receptors (Koh et al., 1995; Swanson et al., 1997), which will result in a larger depolarization. In addition, synaptic responses mediated by GluR2-lacking receptors undergo short-term facilitation to trains of inputs that is due to the relief of polyamine block (Rozov et al., 1998). Hence, the pattern of depolarization integrated by the cell will be distinct depending on the level of GluR2-lacking receptors and will alter the information processing and resulting output of the cell. CARP will also change the pattern and magnitude of synaptic calcium influx and calcium-dependent intracellular signaling that are so critical for synaptic plasticity (Goldberg et al., 2003). CARP is likely to be a common form of plasticity that can regulate both synaptic strength and calcium signaling at excitatory synapses.

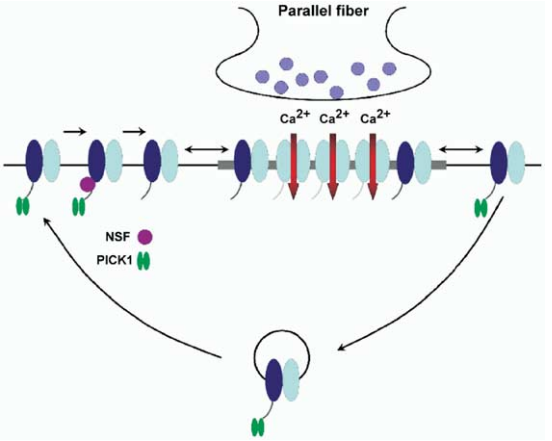

Figure 10. Model of GluR2 Trafficking in Cerebellar Stellate Cells

PICK1 is involved in establishing and maintaining extrasynaptic pools of GluR2-containing receptors both intracellularly and in the plasma membrane. Upon NSF binding to GluR2 and subsequent ATP hydrolysis, PICK1 dissociates from GluR2, and these receptors can then be incorporated into the synaptic membrane. The rates of receptor cycling between intracellular, extrasynaptic, and synaptic locations are dynamically regulated by activity and rely on modulation of protein-protein interactions, most likely by protein phosphorylation/dephosphorylation events.

Experimental Procedures

Animals, Preparation of Slices, and Saline Composition

All experiments were done in accordance with the policies of the Animal Care and Use Committee at the Johns Hopkins School of Medicine. Sprague-Dawley rats and C57/BL6 mice 18–21 days of age were used for all experiments. They were obtained from Harlan and housed in an on-site animal facility at the Johns Hopkins Medical School campus until needed. In addition, transgenic mice (ages 18–21 days old) used for the work in this paper were bred and maintained in an in-house colony. For all transgenic animals, a hybrid genetic background of 129 and C57/BL6 strains was used.

The dissection and slicing of the cerebellum was done in ice-cold, oxygenated physiological saline. Thin slices (200–250 μm) of cerebellar vermis were cut in the sagittal or coronal plane with a vibratome. Slices were allowed to rest on a nylon mesh in oxygenated physiological saline at 37°C for 1 hr and then stored at room temperature until used for recording.

The saline solution for dissections and recording contained the following according to Liu and Cull-Candy (2000): 125 mM NaCl, 2.5 mM KCl, 2 mM $CaCl_2$, 1 mM $MgCl_2$, 26 mM $NaHCO_3$, 1.25 mM

NaH_2PO_4, and 25 mM glucose (pH 7.4). GABAergic inhibition was blocked in all experiments by the addition of 100 μM picrotoxin to the bath saline. Twenty micromolar DL-AP5 was added to the saline to prevent the activation of NMDA receptors.

Patch-Clamp Recording

All recordings were be made at room temperature. Glass patch pipettes for recording (6–10 MΩ) were filled with a caesium-based solution composed of the following: 140 mM $CsMeSO_4$, 10 mM CsHEPES, 10 mM CsEGTA, 2 mM NaCl, 2 mM ATP-Mg, 1 mM QX314, 5 mM TEA, 1 mM $CaCl_2$, 0.1 mM spermine, 0.1 mM bestatin, 0.1 mM leupeptin, and 0.1 mM pepstatin A (pH 7.3). Voltage-clamp experiments were performed using the Axopatch-1C patch-clamp amplifier (Axon Instruments). Data were digitized at 20 kHz and analyzed with pClamp8 software (Axon Instruments). The cesium and QX314 aided in the voltage-clamp of the cell during the recording by blocking many voltage-gated potassium channels and voltage-gated sodium channels, respectively.

Stellate cells are situated in the outer two-thirds of the cell-poor molecular layer of the cerebellar cortex in the path of the axons of the granule cells, the parallel fibers, which provide their excitatory drive (Chan-Palay and Chan-Palay, 1972). Stellate cells fire action potentials spontaneously, and this property seen prior to establishing a whole-cell recording along with their location within the molecular layer can be used to identify them. The input resistance of the neurons was >1 GΩ and therefore no whole-cell capacitance was adjusted and the series resistance was left uncompensated. A glass patch electrode filled with bath saline will be placed in the molecular layer and used to activate one or two synapses onto the stellate cell.

The rectification ratio was calculated as the current measured at +40 mV over the current at –60 mV. This measurement was used to track any changes in the GluR2 content of synaptic AMPA receptors in the presence of peptide or following HFS. CARP was induced by delivering a single, 50 Hz train (300 stimuli) to the parallel fibers.

For all experiments, t = 0 was the time that recording began after establishing a stable recording, usually 3–5 min after entering the whole-cell configuration. The series resistance was monitored throughout the experiment, and cells were discarded if there was a change of >10%. A complete current-voltage relationship (holding potential steps from +60 mV to –60 mV in 20 mV increments) was recorded every 5–10 min throughout recording to verify that there was no drift in the recording (no change in the reversal potential of the evoked AMPA receptor responses).

To measure extrasynaptic AMPA receptor currents, excised somatic patches were positioned in front of the control barrel (100 μM cyclothiazide added to bath saline) of a theta glass pipette. The membrane potential of the patch was stepped to –100 mV and the patch exposed to test solution [100 μM each of cyclothiazide and (RS)-AMPA in bath saline]. The membrane potential was ramped from –100 mV to +80 mV (55.4 mV s^{-1}), and currents were recorded in the presence and absence of agonist. AMPA receptor-mediated currents were the difference between currents evoked by the two ramps. For peptide-disruption experiments, the whole-cell recording was maintained for 15 min prior to patch excision.

Peptides

All peptides were synthesized at an in-house facility. Intracellularly perfused peptides (200 μM) were NSF (KAMKVAKNPQ), NSF control (ARMKVAKNPQ), AP2 (KRMKLNINPS), SVKI (KKEGYNVYG IESVKI), EVKI (KKEGYNVYGIEEVKI), S(PO_4)VKI (KKEGYNVYGIES (PO_4)VKI), SVAI (KKEGYNVYGIESVAI), SGKA (KKEGYNVYGIES GKA), and dynamin (PPPQVPSRPNRAPPG).

Data Analysis

The change in rectification following HFS was quantified using a paired t test. For all peptide experiments, the change in the amplitudes and rectification ratio at the final time point was compared to that at t = 0 min for baseline effects and the time point before HFS for the plasticity using a paired t test. In the experiments with transgenic mice, comparisons of properties to wild-type littermates were done with an unpaired t test.

Supplemental Data

The Supplemental Data that accompanies this article can be found online at http://www.neuron.org/cgi/content/full/45/6/903/DC1/.

Acknowledgments

We would like to thank R. Sattler, J. Steinberg, D. Bergles, and E. Bartlett for critically reading the manuscript. This work was supported by NIH NS43061 (S.M.G.), NIH NS36715 (R.L.H), The Robert Packard Center for ALS Research, MDA's Wings Over Wall Street, and the Howard Hughes Medical Institute. The authors have declared a conflict of interest. For details, see the Supplemental Data.

Received: October 15, 2004
Revised: January 19, 2005
Accepted: February 16, 2005
Published: March 23, 2005

References

Baude, A., Molnar, E., Latawiec, D., McIlhinney, R.A., and Somogyi, P. (1994). Synaptic and nonsynaptic localization of the GluR1 subunit of the AMPA-type excitatory amino acid receptor in the rat cerebellum. J. Neurosci. *14*, 2830–2843.

Bladt, F., Tafuri, A., Gelkop, S., Langille, L., and Pawson, T. (2002). Epidermolysis bullosa and embryonic lethality in mice lacking the multi-PDZ domain protein GRIP1. Proc. Natl. Acad. Sci. USA *99*, 6816–6821.

Bowie, D., and Mayer, M.L. (1995). Inward rectification of both AMPA and kainate subtype glutamate receptors generated by polyamine-mediated ion channel block. Neuron *15*, 453–462.

Braithwaite, S.P., Xia, H., and Malenka, R.C. (2002). Differential roles for NSF and GRIP/ABP in AMPA receptor cycling. Proc. Natl. Acad. Sci. USA *99*, 7096–7101.

Bredt, D.S., and Nicoll, R.A. (2003). AMPA receptor trafficking at excitatory synapses. Neuron *40*, 361–379.

Burnashev, N., Monyer, H., Seeburg, P.H., and Sakmann, B. (1992). Divalent ion permeability of AMPA receptor channels is dominated by the edited form of a single subunit. Neuron *8*, 189–198.

Chan-Palay, V., and Chan-Palay, S.L. (1972). The stellate cells of the rat's cerebellar cortex. Z. Anat. Entwicklungsgesch. *136*, 224–248.

Chung, H.J., Xia, J., Scannevin, R.H., Zhang, X., and Huganir, R.L. (2000). Phosphorylation of the AMPA receptor subunit GluR2 differentially regulates its interaction with PDZ domain-containing proteins. J. Neurosci. *20*, 7258–7267.

Chung, H.J., Steinberg, J.P., Huganir, R.L., and Linden, D.J. (2003). Requirement of AMPA receptor GluR2 phosphorylation for cerebellar long-term depression. Science *300*, 1751–1755.

Collingridge, G.L., Isaac, J.T., and Wang, Y.T. (2004). Receptor trafficking and synaptic plasticity. Nat. Rev. Neurosci. *5*, 952–962.

Daw, M.I., Chittajallu, R., Bortolotto, Z.A., Dev, K.K., Duprat, F., Henley, J.M., Collingridge, G.L., and Isaac, J.T. (2000). PDZ proteins interacting with C-terminal GluR2/3 are involved in a PKC-dependent regulation of AMPA receptors at hippocampal synapses. Neuron *28*, 873–886.

Dev, K.K., Nishimune, A., Henley, J.M., and Nakanishi, S. (1999). The protein kinase C alpha binding protein PICK1 interacts with short but not long form alternative splice variants of AMPA receptor subunits. Neuropharmacology *38*, 635–644.

Donevan, S.D., and Rogawski, M.A. (1995). Intracellular polyamines mediate inward rectification of Ca(2+)-permeable alpha-amino-3-hydroxy-5-methyl-4-isoxazolepropionic acid receptors. Proc. Natl. Acad. Sci. USA *92*, 9298–9302.

Dong, H., O'Brien, R.J., Fung, E.T., Lanahan, A.A., Worley, P.F., and

Huganir, R.L. (1997). GRIP: a synaptic PDZ domain-containing protein that interacts with AMPA receptors. Nature *386*, 279–284.

Goldberg, J.H., Tamas, G., Aronov, D., and Yuste, R. (2003). Calcium microdomains in aspiny dendrites. Neuron *40*, 807–821.

Greger, I.H., Khatri, L., Kong, X., and Ziff, E.B. (2003). AMPA receptor tetramerization is mediated by Q/R editing. Neuron *40*, 763–774.

Groc, L., Heine, M., Cognet, L., Brickley, K., Stephenson, F.A., Lounis, B., and Choquet, D. (2004). Differential activity-dependent regulation of the lateral mobilities of AMPA and NMDA receptors. Nat. Neurosci. *7*, 695–696.

Hanley, J.G., Khatri, L., Hanson, P.I., and Ziff, E.B. (2002). NSF ATPase and alpha-/beta-SNAPs disassemble the AMPA receptor-PICK1 complex. Neuron *34*, 53–67.

Hollmann, M., O'Shea-Greenfield, A., Rogers, S.W., and Heinemann, S. (1989). Cloning by functional expression of a member of the glutamate receptor family. Nature *342*, 643–648.

Hollmann, M., Hartley, M., and Heinemann, S. (1991). Ca2+ permeability of KA-AMPA–gated glutamate receptor channels depends on subunit composition. Science *252*, 851–853.

Kamboj, S.K., Swanson, G.T., and Cull-Candy, S.G. (1995). Intracellular spermine confers rectification on rat calcium-permeable AMPA and kainate receptors. J. Physiol. *486*, 297–303.

Kim, C.H., Chung, H.J., Lee, H.K., and Huganir, R.L. (2001). Interaction of the AMPA receptor subunit GluR2/3 with PDZ domains regulates hippocampal long-term depression. Proc. Natl. Acad. Sci. USA *98*, 11725–11730.

Koh, D.S., Burnashev, N., and Jonas, P. (1995). Block of native Ca(2+)-permeable AMPA receptors in rat brain by intracellular polyamines generates double rectification. J. Physiol. *486*, 305–312.

Lee, S.H., Liu, L., Wang, Y.T., and Sheng, M. (2002). Clathrin adaptor AP2 and NSF interact with overlapping sites of GluR2 and play distinct roles in AMPA receptor trafficking and hippocampal LTD. Neuron *36*, 661–674.

Lee, S.H., Simonetta, A., and Sheng, M. (2004). Subunit rules governing the sorting of internalized AMPA receptors in hippocampal neurons. Neuron *43*, 221–236.

Li, P., Kerchner, G.A., Sala, C., Wei, F., Huettner, J.E., Sheng, M., and Zhuo, M. (1999). AMPA receptor-PDZ interactions in facilitation of spinal sensory synapses. Nat. Neurosci. *2*, 972–977.

Liu, S.Q., and Cull-Candy, S.G. (2000). Synaptic activity at calcium-permeable AMPA receptors induces a switch in receptor subtype. Nature *405*, 454–458.

Liu, S.J., and Cull-Candy, S.G. (2002). Activity-dependent change in AMPA receptor properties in cerebellar stellate cells. J. Neurosci. *22*, 3881–3889.

Lledo, P.M., Zhang, X., Sudhof, T.C., Malenka, R.C., and Nicoll, R.A. (1998). Postsynaptic membrane fusion and long-term potentiation. Science *279*, 399–403.

Lomeli, H., Mosbacher, J., Melcher, T., Hoger, T., Geiger, J.R., Kuner, T., Monyer, H., Higuchi, M., Bach, A., and Seeburg, P.H. (1994). Control of kinetic properties of AMPA receptor channels by nuclear RNA editing. Science *266*, 1709–1713.

Luscher, C., Xia, H., Beattie, E.C., Carroll, R.C., von Zastrow, M., Malenka, R.C., and Nicoll, R.A. (1999). Role of AMPA receptor cycling in synaptic transmission and plasticity. Neuron *24*, 649–658.

Luthi, A., Chittajallu, R., Duprat, F., Palmer, M.J., Benke, T.A., Kidd, F.L., Henley, J.M., Isaac, J.T., and Collingridge, G.L. (1999). Hippocampal LTD expression involves a pool of AMPA receptors regulated by the NSF-GluR2 interaction. Neuron *24*, 389–399.

Matsuda, S., Mikawa, S., and Hirai, H. (1999). Phosphorylation of serine-880 in GluR2 by protein kinase C prevents its C terminus from binding with glutamate receptor-interacting protein. J. Neurochem. *73*, 1765–1768.

Mosbacher, J., Schoepfer, R., Monyer, H., Burnashev, N., Seeburg, P.H., and Ruppersberg, J.P. (1994). A molecular determinant for submillisecond desensitization in glutamate receptors. Science *266*, 1059–1062.

Nishimune, A., Isaac, J.T., Molnar, E., Noel, J., Nash, S.R., Tagaya, M., Collingridge, G.L., Nakanishi, S., and Henley, J.M. (1998). NSF binding to GluR2 regulates synaptic transmission. Neuron *21*, 87–97.

Noel, J., Ralph, G.S., Pickard, L., Williams, J., Molnar, E., Uney, J.B., Collingridge, G.L., and Henley, J.M. (1999). Surface expression of AMPA receptors in hippocampal neurons is regulated by an NSF-dependent mechanism. Neuron *23*, 365–376.

Osten, P., Srivastava, S., Inman, G.J., Vilim, F.S., Khatri, L., Lee, L.M., States, B.A., Einheber, S., Milner, T.A., Hanson, P.I., and Ziff, E.B. (1998). The AMPA receptor GluR2 C terminus can mediate a reversible, ATP-dependent interaction with NSF and alpha- and beta-SNAPs. Neuron *21*, 99–110.

Osten, P., Khatri, L., Perez, J.L., Kohr, G., Giese, G., Daly, C., Schulz, T.W., Wensky, A., Lee, L.M., and Ziff, E.B. (2000). Mutagenesis reveals a role for ABP/GRIP binding to GluR2 in synaptic surface accumulation of the AMPA receptor. Neuron *27*, 313–325.

Passafaro, M., Piech, V., and Sheng, M. (2001). Subunit-specific temporal and spatial patterns of AMPA receptor exocytosis in hippocampal neurons. Nat. Neurosci. *4*, 917–926.

Perez, J.L., Khatri, L., Chang, C., Srivastava, S., Osten, P., and Ziff, E.B. (2001). PICK1 targets activated protein kinase C-alpha to AMPA receptor clusters in spines of hippocampal neurons and reduces surface levels of the AMPA-type glutamate receptor subunit 2. J. Neurosci. *21*, 5417–5428.

Peter, B.J., Kent, H.M., Mills, I.G., Vallis, Y., Butler, P.J., Evans, P.R., and McMahon, H.T. (2004). BAR domains as sensors of membrane curvature: the amphiphysin BAR structure. Science *303*, 495–499.

Petralia, R.S., Wang, Y.X., Mayat, E., and Wenthold, R.J. (1997). Glutamate receptor subunit 2-selective antibody shows a differential distribution of calcium-impermeable AMPA receptors among populations of neurons. J. Comp. Neurol. *385*, 456–476.

Rozov, A., Zilberter, Y., Wollmuth, L.P., and Burnashev, N. (1998). Facilitation of currents through rat Ca2+-permeable AMPA receptor channels by activity-dependent relief from polyamine block. J. Physiol. *511*, 361–377.

Shi, S., Hayashi, Y., Esteban, J.A., and Malinow, R. (2001). Subunit-specific rules governing AMPA receptor trafficking to synapses in hippocampal pyramidal neurons. Cell *105*, 331–343.

Sommer, B., Keinanen, K., Verdoorn, T.A., Wisden, W., Burnashev, N., Herb, A., Kohler, M., Takagi, T., Sakmann, B., and Seeburg, P.H. (1990). Flip and flop: a cell-specific functional switch in glutamate-operated channels of the CNS. Science *249*, 1580–1585.

Sommer, B., Kohler, M., Sprengel, R., and Seeburg, P.H. (1991). RNA editing in brain controls a determinant of ion flow in glutamate-gated channels. Cell *67*, 11–19.

Song, I., Kamboj, S., Xia, J., Dong, H., Liao, D., and Huganir, R.L. (1998). Interaction of the N-ethylmaleimide-sensitive factor with AMPA receptors. Neuron *21*, 393–400.

Song, I., and Huganir, R.L. (2002). Regulation of AMPA receptors during synaptic plasticity. Trends Neurosci. *25*, 578–588.

Srivastava, S., Osten, P., Vilim, F.S., Khatri, L., Inman, G., States, B., Daly, C., DeSouza, S., Abagyan, R., Valtschanoff, J.G., et al. (1998). Novel anchorage of GluR2/3 to the postsynaptic density by the AMPA receptor-binding protein ABP. Neuron *21*, 581–591.

Steinberg, J.P., Huganir, R.L., and Linden, D.J. (2004). N-ethylmaleimide-sensitive factor is required for the synaptic incorporation and removal of AMPA receptors during cerebellar long-term depression. Proc. Natl. Acad. Sci. USA *101*, 18212–18216.

Swanson, G.T., Kamboj, S.K., and Cull-Candy, S.G. (1997). Single-channel properties of recombinant AMPA receptors depend on RNA editing, splice variation, and subunit composition. J. Neurosci. *17*, 58–69.

Takamiya, K., Kostourou, V., Adams, S., Jadeja, S., Chalepakis, G., Scambler, P.J., Huganir, R.L., and Adams, R.H. (2004). A direct functional link between the multi-PDZ domain protein GRIP1 and the Fraser syndrome protein Fras1. Nat. Genet. *36*, 172–177.

Tardin, C., Cognet, L., Bats, C., Lounis, B., and Choquet, D. (2003). Direct imaging of lateral movements of AMPA receptors inside synapses. EMBO J. *22*, 4656–4665.

Terashima, A., Cotton, L., Dev, K.K., Meyer, G., Zaman, S., Duprat,

F., Henley, J.M., Collingridge, G.L., and Isaac, J.T. (2004). Regulation of synaptic strength and AMPA receptor subunit composition by PICK1. J. Neurosci. *24*, 5381–5390.

Wang, Y.T., and Linden, D.J. (2000). Expression of cerebellar long-term depression requires postsynaptic clathrin-mediated endocytosis. Neuron *25*, 635–647.

Wenthold, R.J., Petralia, R.S., Blahos, J., II, and Niedzielski, A.S. (1996). Evidence for multiple AMPA receptor complexes in hippocampal CA1/CA2 neurons. J. Neurosci. *16*, 1982–1989.

Xia, J., Zhang, X., Staudinger, J., and Huganir, R.L. (1999). Clustering of AMPA receptors by the synaptic PDZ domain-containing protein PICK1. Neuron *22*, 179–187.

Xia, J., Chung, H.J., Wihler, C., Huganir, R.L., and Linden, D.J. (2000). Cerebellar long-term depression requires PKC-regulated interactions between GluR2/3 and PDZ domain-containing proteins. Neuron *28*, 499–510.

Zimmerberg, J., and McLaughlin, S. (2004). Membrane curvature: how BAR domains bend bilayers. Curr. Biol. *14*, R250–R252.